Personalized Bistable Orthoses for Rehabilitation of Finger Joints

Yuyu Lin
Human-Computer Interaction Institute, Carnegie Mellon University
Pittsburgh, PA, USA
yuyulin@andrew.cmu.edu

Dian Zhu
Carnegie Mellon University
Pittsburgh, PA, USA
dianz@andrew.cmu.edu

Anoushka Naidu
Carnegie Mellon University
Pittsburgh, PA, USA
anaidu@andrew.cmu.edu

Kenneth Yu
Carnegie Mellon University
Pittsburgh, PA, USA
ky2@andrew.cmu.edu

Deon Harper
Carnegie Mellon University
Pittsburgh, PA, USA
dharper@andrew.cmu.edu

Eni Halilaj
Mechanical Engineering Department
Carnegie Mellon University
Pittsburgh, PA, USA
ehalilaj@andrew.cmu.edu

Douglas Weber
Mechanical Engineering Department
Carnegie Mellon University
Pittsburgh, PA, USA
dweber2@andrew.cmu.edu

Deborah Kenney
Department of Orthopaedic Surgery
Stanford University
Redwood City, CA, USA
dkenney@stanford.edu

Adam J. Popchak
Department of Physical Therapy
University of Pittsburgh
Pittsburgh, PA, USA
ajp64@pitt.edu

Mark Baratz
University of Pittsburgh Medical Center
Pittsburgh, PA, USA
baratzme@upmc.edu

Alexandra Ion
Human-Computer Interaction Institute, Carnegie Mellon University
Pittsburgh, PA, USA
alexandraion@cmu.edu

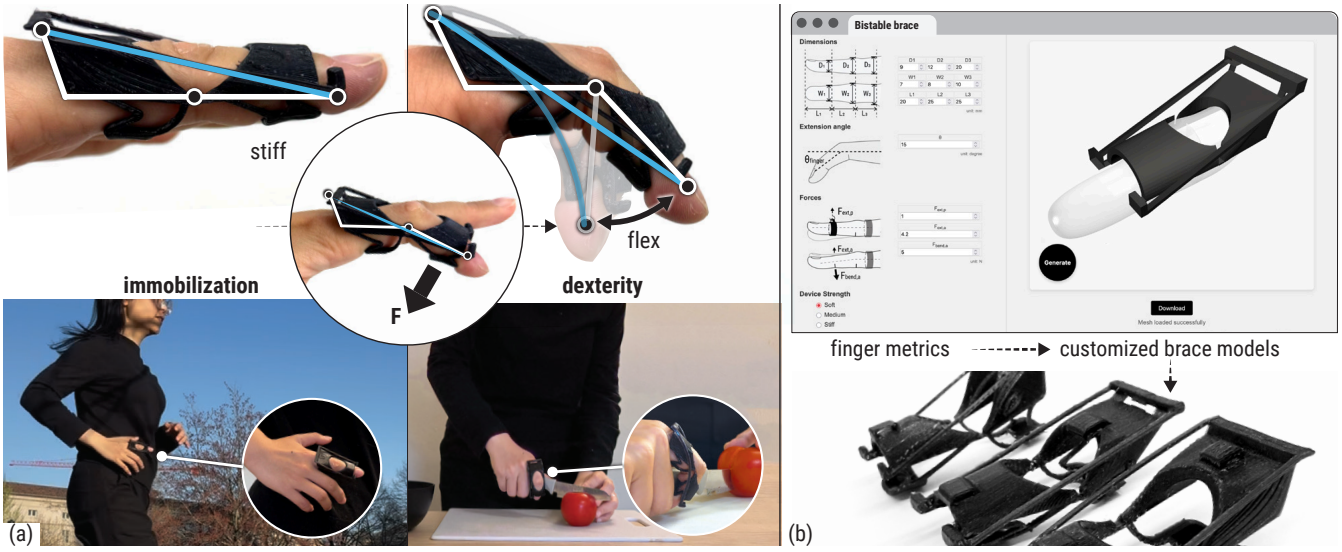

Figure 1: We present the design of a bistable brace that (a) enables easy switching between immobilization, when the hands are not actively used (e.g., running), and dexterity, when the hands are in active use (e.g., cutting vegetables). (b) Our customization design pipeline generates 3D-printable models tailored to individual finger metrics, including finger strengths.

Abstract

Orthoses are essential components of rehabilitation, yet limited in functionality. Static braces immobilize joints, which, especially for hand and finger injuries, interfere with users' daily activities. Additionally, early mobilization schedules require users to take off and reapply their static orthoses frequently, which is cumbersome.

To facilitate both *rehabilitation* and *dexterity*, we introduce a novel multifunctional yet unpowered finger orthosis design. Our design supports easy switching between two distinct states: a stiff state for immobilization and a flexible state for mobilization. A key benefit is that it can be customized using our computational design tool, and 3D printed in one piece. Our computational design pipeline supports tailoring the switching thresholds of the brace based on patients' individual finger strengths and range of motion. Following a preliminary study with 10 healthy people that validates the usability and wearability of the brace, our two-week case study with a patient indicates that our brace supports everyday activities and assists with rehabilitation.

CCS Concepts

• **Human-centered computing → Human computer interaction (HCI)**.

Keywords

Unpowered Orthosis, Compliant Mechanism, Bistable Structure, Stiffness-tunable Materials

ACM Reference Format:

Yuyu Lin, Dian Zhu, Anoushka Naidu, Kenneth Yu, Deon Harper, Eni Halilaj, Douglas Weber, Deborah Kenney, Adam J. Popchak, Mark Baratz, and Alexandra Ion. 2025. Personalized Bistable Orthoses for Rehabilitation of Finger Joints. In *The 38th Annual ACM Symposium on User Interface Software and Technology (UIST '25), September 28–October 01, 2025, Busan, Republic of Korea.* ACM, New York, NY, USA, 18 pages. https://doi.org/10.1145/3746059.3747643

1 INTRODUCTION

Customization is crucial for wearable devices to ensure comfort, functionality, and user compliance. Digital fabrication excels in enabling such customization. Through computational design, tailored geometries can be generated and 3D printed to conform to the unique bodies of users. Personalization is even more critical for injured body parts, which are typically sensitive to movement and restricted in strength and range of motion due to specific conditions (e.g., injury, inflammation, dislocations). HCI researchers have acknowledged this user group (i.e., patients) and applied their expertise to innovate rehabilitation devices. Examples include sensor-integrated textile covers for prosthetic limbs [26], moldable rigid orthoses with embedded electronics [36] and sensing [50], or robotic devices for finger compression therapy [22].

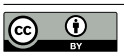

UIST '25, Busan, Republic of Korea

ACM ISBN 979-8-4007-2037-6/25/09
https://doi.org/10.1145/3746059.3747643

Among all rehabilitation tasks, hand rehabilitation particularly demands personalization because the hands are typically involved in many daily activities, so even minor dexterity limitations can significantly affect daily function and independence. Hand injuries account for up to 20% of all emergency room visits and represent the most frequent occupational injury treated in the U.S. [8]. Many hand injuries affect finger joints and their tendons, for which orthoses (also known as splints, see Figure 2a) are often prescribed to immobilize the joints during healing [12] and help restore or maintain range of motion [7].

Maintaining a balance between immobilizing the hand and actively using the hand is key to recovery [12, 45], but it is hard to integrate this routine seamlessly into users' daily activities [20, 44]. For example, to use the finger for, e.g., 1 hour every 3 hours (exact times depend on the individual cases), patients using a static brace have to remove it many times a day and put it back on. This cumbersome routine often frustrates patients [44] as patients struggle to manage hand exercise while keeping the finger well protected [20, 44]. Some forget to put their braces back on [38], while others over-immobilize out of caution or pain [44], which may result in poor therapeutic outcomes, such as long-term stiffness and reduced range of motion [6]. A simple and pain-free solution is needed that supports patients in adhering to their recommended rehabilitation routine.

In this paper, we present a novel finger brace that eliminates the drawbacks of intermittent use of a static brace by *combining immobilization and mobilization into one personalized brace*, without requiring external power. Our bistable brace, shown in Figure 2b, allows patients to switch between a *stiff state* for immobilization and a *flexible state* where they can freely flex their finger for mobilization, without taking the brace off. This supports patients to follow their rehabilitation regimen and perform daily activities (Figure 2c). To switch between these states, users simply intentionally bend their finger. Switching from the stiff state to the flexible state, users simply flex their fingers. To switch from the flexible back into the stiff state, users extend their fingers.

Our brace is personalized to the patient (joint strength, extension angle, finger dimensions), which is enabled by our custom computational design tool.

1.1 Working Principle

We designed our brace as a compliant bistable mechanism. In Figure 1, we show an example of a patient with an injury to the PIP joint of the index finger, i.e., the middle joint of their finger. In the *stiff state*, the user's finger is held in a stable position, allowing their joint to rest. Users may keep it in this state during activities that don't require dexterity, e.g., in social settings, while taking a walk, etc. In the *flexible state*, users can combine their mobilization schedule with dexterous daily tasks like chopping vegetables, doing household chores, etc. The force needed to switch from stiff to flexible is set below the user's measured strength to ensure that they are capable of switching the state intentionally without accidental triggering.

When users want to switch from the flexible state back to the stiff state, they extend their finger as far as they can. We measure their maximum extension angle and set the angle at which the brace

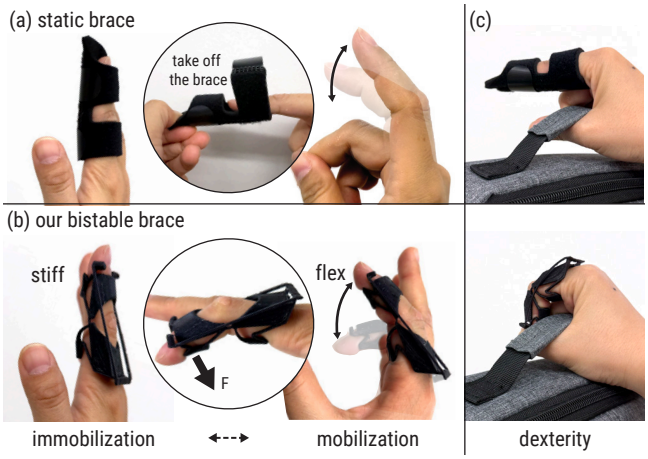

Figure 2: The rehabilitation routine of (a) using a static brace that immobilizes the finger, which requires removing the brace for active mobilization exercises; and (b) by naturally switching between immobilization and mobilization with our brace, by just bending the finger. (c) Dexterity is limited when using a static brace, whereas our design supports active finger use during daily tasks, such as grasping.

snaps to the stiff state just below that. As the brace snaps to the stiff state, it creates a pulling force that pulls the user's finger into a straight position. Along with the user's finger dimensions, we use these three measured parameters, i.e., (1) user's pushing down force, (2) their maximum extension angle, and (3) their joint stiffness, as input to our computational design tool. Our tool then optimizes the single-piece 3D printable brace with appropriate forces for each user's needs.

1.2 Contributions

Our core contribution is a novel parametric, bistable finger brace design that enables users to easily switch between performing dexterous activities and rehabilitation. Specifically, we make the following contributions:

(1) We present the *monolithic geometry design* of a multifunctional yet unpowered orthosis.
(2) We characterize how key geometric parameters can be adjusted to match users' finger strengths and extension angle through a *technical evaluation.*
(3) We further introduce a *computational design pipeline* that generates personalized brace models based on user-specific parameters.
(4) We validate the dual functionality and usability of our brace through a preliminary *wearability study* with 10 healthy participants, demonstrating that our brace supports both immobilization and dexterous tasks such as grasping and writing.
(5) Following this, we conduct a *case study* with a patient over a two-week period, to evaluate our brace's impact on daily living and rehabilitation journey.

Our work is situated within HCI fabrication research as we contribute a new artifact (a novel 3D printed brace design) for specific users (patients with joint injuries) and a design tool for physicians to customize it. While there could be broader application potential for our wearable device, e.g., as an exoskeleton, we intentionally focus our application narrowly on rehabilitation. This paper is not intended to generalize and explore applications, but to solve a specific, important problem for users in joint rehabilitation.

2 RELATED WORK

Our work builds on previous work in personal and user-centered rehabilitation devices, bistable mechanisms, and customized, multifunctional orthoses.

2.1 Personal Fabrication for Rehabilitation

Customizable and interactive rehabilitation devices have been an important area in human-computer interaction (HCI). Prior research has explored various aspects of device fabrication [30], monitoring [21, 51, 58], sensing [26], and tangible interactions [24, 31] to support rehabilitation.

By enabling tailored rehabilitation, personal fabrication techniques empower both end-users [15, 17, 41] and clinicians [16]. Supporting users in creating their own assistive technologies has been shown to improve adoption rates [17]. Nowadays, 3D printing technology is increasingly popular in personal orthopedic fabrication [1, 33, 40], which supports easy customization and rapid prototyping.

Building on this goal of empowerment and personalization, our work provides a customizable, adaptive solution for users' finger rehabilitation.

2.2 Bistable Mechanism Applications

Bistable structures have been widely explored, due to their unique snap-through behavior and the benefit of the maintenance of two stable configurations without requiring continuous energy input [5]. Applications include shape-changing interfaces composed of deployable structures [10, 28, 34], materials with tunable properties [29, 57], soft robots with bistable actuation [4, 35] and digital mechanical metamaterials [18, 19]. To the best of our knowledge, this work is the first to investigate monolithic bistable structures for rehabilitation.

2.3 Orthosis Customization

Researchers have been exploring computational design methods that show promise in achieving precise body conformity, using techniques such as thermoforming [36, 50] and casting [27, 56]. For example, Zhang et al. [55] proposed a pipeline to produce thermal-comfort and personalized orthopedic casts. To fabricate customizable orthoses through 3D printing [33, 40], Wang et al. [50] introduced a pipeline that enables both shape and electronics placement to conform to individual bodies. These approaches focus on static braces, highlighting the importance of on-body personalization of orthotic devices.

Dynamic braces are a type of braces that allow movement while applying corrective force on the finger joint [3]. Adjustable dynamic braces have been developed to allow users to manually change the

corrective force of the device [37]. They are typically mass-produced and rely on fixed-tension, large spring force. Due to the inherent spring properties, the range of adjustable strengths is predefined.

To support user-specific customization based on individual strengths, in this paper, we propose a design pipeline for a multifunctional orthosis. This enables a rehabilitation routine that combines both the immobilization and mobilization phases.

2.4 Multi-Functional Orthoses

Researchers have explored robotic and actuated exoskeletons that adapt to users' daily needs through motorized [39, 49] or pneumatic actuations [9, 30]. In HCI research, VR gloves also apply forces for haptic feedback, enhancing virtual interactions [13, 14, 47]. These devices are also powered exoskeletons. For example, SomatoShift [14] integrates mechanical articulation with feedback mechanisms to provide realistic sensory experiences, such as modifying the ease of movement.

In this paper, we emphasize a highly customizable and simple solution, without relying on bulky actuators or external power sources, which increase complexity and reduce wearability. To support patients' everyday lives and long-term rehabilitation, we propose a fully passive orthosis that supports dual functionalities.

3 BACKGROUND

In this section, we introduce the multiple stakeholders involved in our design process and the two main rehabilitation scenarios that we focus on.

3.1 Multiple Stakeholders in the Design Process

This interdisciplinary collaboration integrates expertise from HCI, biomechanics, and clinical research. The HCI researchers initiated the project, designed the mechanism, and conducted the evaluations. The biomechanics experts supported this process by identifying critical metrics and technical evaluation protocols. Our collaborators evaluated early prototypes of the brace and provided feedback based on the rehabilitation requirements and their experience with patient care, which informed key design decisions, particularly around assistive forces and wearability, ensuring relevance to clinical practice. The medical experts on the team included a hand orthopedic surgeon, a physical therapist, an occupational therapist (all from the University of Pittsburgh Medical Center), and a research scientist for hand-related research from Stanford University School of Medicine. We developed the protocol for our case study with a patient (Section 9) and reviewed the results with the clinicians on the team, ensuring that it is aligned with clinical practice and captures meaningful outcomes.

Our medical collaborators provided insight into our target patient populations, rehabilitation timelines, and requirements. Among various finger joint conditions (e.g., arthritis, contractures, fractures), they identified tendon injury rehabilitation [45] for proximal interphalangeal (PIP) joint as the most suitable focus, due to the challenges of treating post-injury stiffness without adequate early mobilization [42, 53]. Specifically, two indications will potentially benefit from a device that supports both protective immobilization and periodic mobilization, as described in the following.

3.2 Supporting Early Mobilization

Similarly to the rehabilitation routine described in the Introduction, the patients' fingers after tendon injuries are typically immobilized for the first few weeks. As healing progresses, they transition to alternating between wearing the brace to allow the tendon 'to grow' and performing controlled exercises without it to prevent long-term finger stiffness [42, 53] in a day. The patients' fingers may still have a full range of motion in extension, they may be limited in flexion, and their joints are typically sore and swollen. As mentioned, repeatedly taking off and putting on their static braces is cumbersome and can disrupt their daily life and cause patients to follow their therapy less consistently [44]. Since tendon rehabilitation can take several weeks to months, creating comfortable braces that do not frequently need to be removed can improve patient compliance and recovery outcomes. Therefore, we anticipate that our brace can help these patients adhere to a regular exercise schedule by supporting easy switching between immobilization and mobilization.

3.3 Limited Motion Range Due to Extensor Lag

Another indication is known as extensor lag, which limits patients' active range of motion. As illustrated in Figure 3, the affected fingers remain bent; that is, patients cannot fully extend their fingers by themselves. However, the finger can still be straightened passively using the other hand, as we illustrate in Figure 3b. This is due to an asymmetry between the extensor and flexor tendon strength, where the extensor tendon is too weak to overcome the flexor tendon. Extensor lag can be caused by tendon rupture or traumatic elongation.

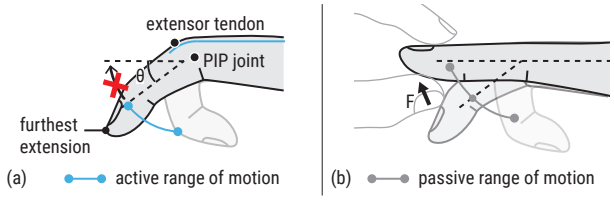

Figure 3: An illustration of a finger joint with extensor lag, which has (a) a limited active range of motion, but (b) with external assistance, can be manipulated through the full range of motion (passive range of motion). (a) The angle between the furthest reachable position and the fully extended position is denoted as the furthest reachable angle, or extension angle θ.

In addition, flexor lag is the opposite issue of extensor lag, i.e., the patient cannot fully bend their fingers into a fist independently, but their fingers can be bent passively. Since extensor tendon injuries are more common than flexor tendon injuries [2], with the index finger representing the most commonly injured finger [8], we will demonstrate our bistable brace on extensor tendon rehabilitation.

For effective rehabilitation, braces in these cases need to position the finger beyond the range that the patient can actively achieve, to help gradually restore the full range of motion. Our bistable brace may be beneficial for this patient group, as it can actively pull fingers when it transitions between its states, beyond the patients' active motion range. Additionally, we can design our brace's angle in the

stiff state and its transition angle independently (see Figure 6c) to adjust to the patient's individual range of motion and rehabilitation needs.

3.4 Current Splints in Practice

As discussed, patients recovering from tendon injuries are most often prescribed static braces, which immobilize the injured joint to protect the healing tissue. The aforementioned dynamic splints are rarely used in practice for both of the above indications [52]. The reason is that their designs don't align well with rehabilitation routines of alternating between periods of immobilization and active mobilization. In addition, dynamic splints typically apply significant force to injured joints, which can cause discomfort or pain [48].

4 BISTABLE ORTHOSIS

Based on the rehabilitation needs for the aforementioned tendon injuries, we derive a set of **design goals**:

- **Easy switching** between immobilization & mobilization, allowing patients to conduct daily activities or doctor's suggested exercise without removing the brace.
- **Customizable range of motion** such that the finger can be extended beyond its active range of motion during immobilization.
- **Customizable stiffness** of the brace to not cause excessive stress on the injured joint.
- **Customizable fit** to ensure effective transmission of forces from the brace and to avoid skin breakdown during wear.

To achieve these goals without actuation, we leverage structural bistability. Our design takes the bent position for daily activities and the extended position for rehabilitation as two stable states. We make it a monolithic, compliant design that further supports customization.

4.1 Easy Switching Mechanism

Bistable mechanisms can hold to distinct states without external force [5]. We use this general mechanism to design our brace, as we illustrate in Figure 4. The brace has two rigid members that are connected by a stiff elastic band. As shown in Figure 4b, when users bend their finger, they rotate the rigid members, eventually causing them to form a line. The elastic band resists this deformation and stretches slightly before the rigid members can snap through and bend further. In other words, it acts similarly to an extension spring. Once snapped through, further rotation causes only little resistance, as the thin band bends very easily (see Figure 4c). As shown in Figure 4d, during the bending process, users must overcome a force threshold F_{down}, and the transition to the flexible region begins at approximately $2 \cdot \theta$, as defined by the geometry of our design.

When returning, the mechanism stretches the elastic band until the structure reaches the critical point, snaps through, and locks itself in the extended position (Figure 5). During extending the finger, the maximum force users should exert is $|F_{\text{up}}|$, and as long as the bending angle θ is passed, the device snaps and pulls the finger into extension.

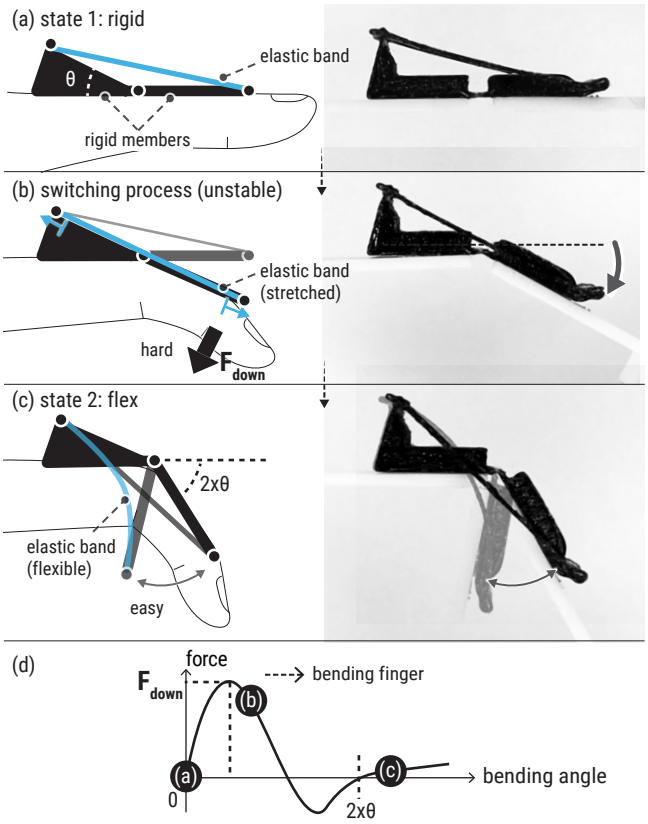

Figure 4: Illustrations of the switching process during finger flexion. (a) The brace starts in the *stiff* state; (b) finger applies a force to reach the switching threshold, which slightly stretches the orthosis elastic band; and (c) the orthosis snaps to its *flex* state, where further rotation is easy. (d) The required finger force during this process changes with the bending angle.

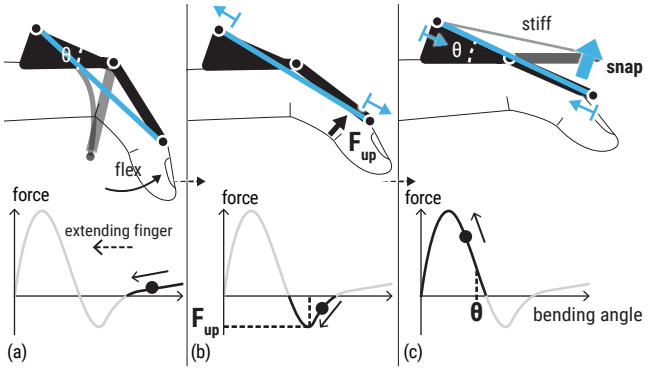

Figure 5: Illustration of the switching process during extension. (a) The finger starts in the *flex* state; (b) a force is applied to reach the switching threshold; and (c) passing a critical angle, the orthosis snaps into the *stiff* state.

4.2 Customizable Design

We can tune the forces and angle that need to be reached to trigger snapping through geometric parameters, allowing customization, as we illustrate in Figure 6. These forces the brace takes to snap between *stiff* and *flex* states are mainly defined by the length of the band in relation to the lengths of the rigid members, which is a geometric property in our design. The switching angle θ_{switch} is also defined by the structure, as it is always a bit larger than the supplementary angle θ between the two rigid-body edges (Figure 6a).

Although these are the most impactful parameters, we note that the compliant hinges connecting the rigid members and the elastic band (illustrated as dots in Figure 6a) also influence the switching angle and forces. We discuss, simulate, and optimize these design parameters in our computational design tool (Section 8.3).

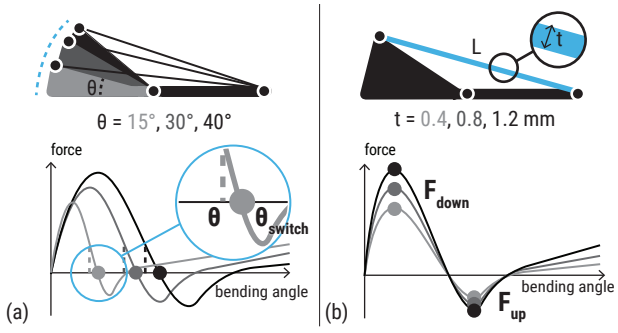

Figure 6: The geometry of our bistable orthosis can be tuned to (a) adjust the switching angle, or (b) adjust the maximum forces required to switch the brace.

4.3 Fabrication

For easy customization, we design our structure to be fully compliant such that it can be 3D printed in one piece without the need for assembly. We print all our prototypes using PCTPE filament, a co-polymer composed of nylon and thermoplastic elastomer. We use PCTPE because of its balance of rigidity, flexibility, and durability based on our early tests. Nylon is widely used in wearables due to its durability and biocompatibility, and PCTPE is particularly good for engineering the elastic band as a tension spring, with 497% elongation at break (X-Y direction). All prototypes in this paper were printed using an Ultimaker 2+ with a 0.4mm nozzle at 60% infill density.

5 TECHNICAL EVALUATION

With a bistable mechanism that enables easy switching, our technical evaluation is to understand how to adjust geometric parameters to user-specific strengths and extension angle, which is crucial for customization.

5.1 Understanding the Geometry-Torque Relationship

First, we aimed to characterize the relationship between geometry and the force thresholds it creates. To do so, we generated different designs and measured the torques needed for *stiff→flex* and *flex→stiff* transitions.

5.1.1 Defining parameters. We denote the parameters of our design as illustrated in Figure 7. Specifically, θ defines the angle at which the mechanism is already in the process of snapping from flex to stiff states. We define θ in our design by construction to match users' capabilities. The force it takes to switch between the states will be defined by the triangle formed by rigid links a and c, which together with θ define the original length L of the elastic band.

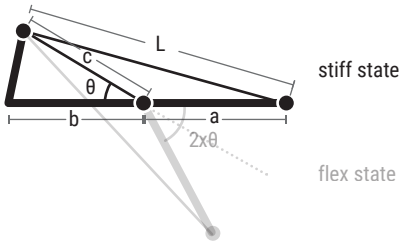

Figure 7: The geometric parameters of our orthotic device.

To establish a model on how the geometry defines the force thresholds, we first generated 14 designs, illustrated in Figure 8, by varying a and c individually to 15, 20, 30, 40, and 50 mm, while keeping the respective other members and b at 20 mm and θ at 30°. Our original parameter range was 10 - 50 mm with 10 mm increments. However, the printed samples with 10 mm length for a and c were not bistable; therefore, we used 15 mm as the lower end. Additionally, we tested the impact of θ using 15°, 30°, 40°, and 45°. As expected, $2 \cdot \theta$ is the start of the flex state (Figure 8b). Larger angles would push the finger in a highly bent position in the flex state, such that users couldn't use their finger effectively anymore, making them infeasible designs.

5.1.2 Measuring torque. To evaluate the effect that the brace would have on a person's PIP joint, we measured our samples on a universal testing machine (Mark-10 ESM 303 and a 50 N force sensor with 0.02 N resolution). As shown in Figure 9, we fixed our samples in a jig close to the flexure where a and c meet. To measure how much torque is needed to switch the brace sample *stiff→flex*, we moved the gauge downwards until the brace sample switched over (see Figure 9a). We compute the maximum downward (bending) torque as $T_{\text{down}} = F_{\perp} * d = F * d_0$. Our jig sets $d_0 = 55mm$. To measure the torque needed to transition *flex→stiff*, we show in Figure 9b how we flipped the brace over in our jig and pushed it down until it switched to its straight position. Here, $d_0 = 10mm$ for our computation of the upward torque (extension) magnitude $|T_{\text{up}}|$. We combined the torque-displacement curves from these two measurements by flipping the displacement of the *flex→stiff* process. We showed the results of a sample with $a = b = 20$, $c = 50$, $\theta = 30$ in Figure 9c. From the torque-displacement curve, the maximum torque is what we want to define with geometry parameters to

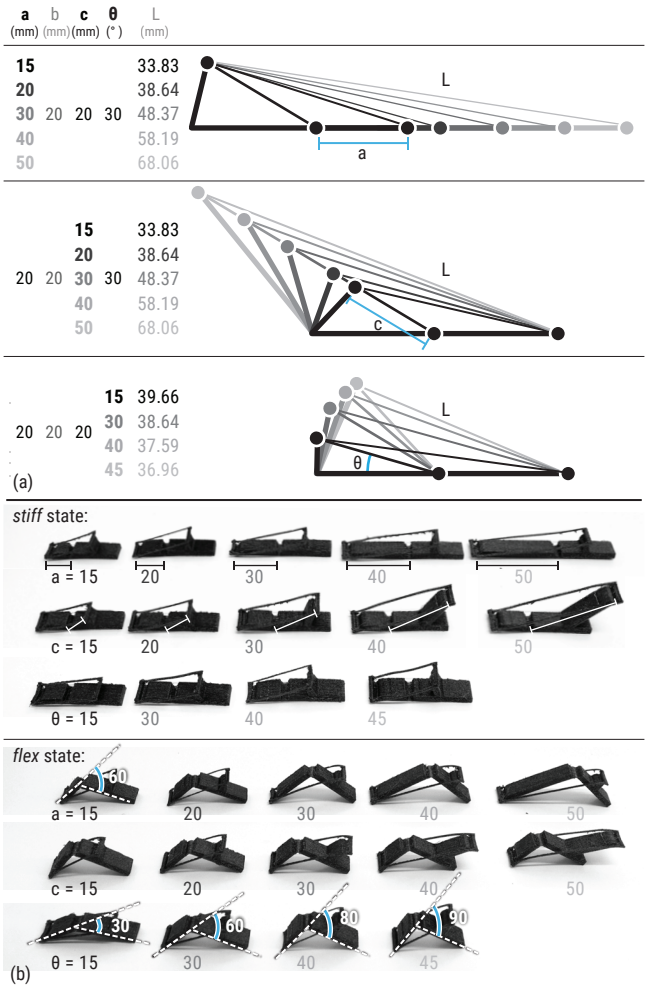

Figure 8: Brace samples for defining key geometric parameters. (a) Illustrations of variations with different a, c and θ. (b) 3D printed samples annotated with the starting angles of the flex state.

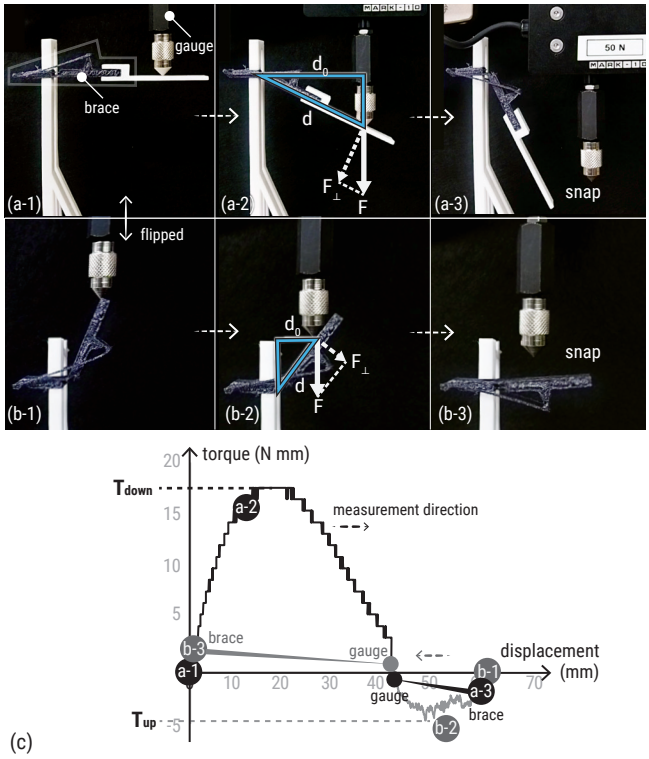

Figure 9: We measured the compression force to switch the states of our sample from (a) extended to bent and (b) from bent to extended. (c) We combined the results of these two measurements to form the torque-displacement curve of the full switching process.

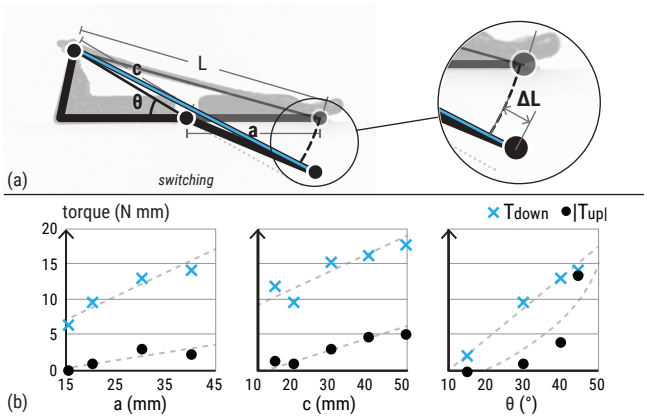

Figure 10: (a) Illustrations of ΔL and (b) the results of how individual parameters a, c, and θ influence the torques.

tune to individual (remaining) strength and to avoid accidental activation. The minimum torque, which is negative, is the force required to pull the finger up to the extended position.

5.1.3 Results. After evaluating multiple models, we found that the torque thresholds correlate with ΔL, that is $a + c - L$, as shown in Figure 10. ΔL is the amount that the elastic band needs to stretch during the snap-through from one stable state into the other, since a and c are collinear at that point. We note that ΔL is an absolute value and depends on the material properties. We expect materials that are easier to stretch than our PCTPE will require a design with a larger ΔL for the same switching torque, and vice versa for more rigid materials.

5.1.4 Varying torque independently. After establishing the correlation between ΔL and the switching torques, we further evaluated the model. We printed 11 new samples of our brace, all with a consistent $\theta = 30°$. We sampled ΔL between 1 and 3 mm in increments of 0.2mm. To do so, we scaled a and c proportionally, as we show in Figure 11. We measured the samples using the same setup and

procedure as before. Our results show that the switching torque grows quadratically with ΔL for both T_{down} and T_{up}.

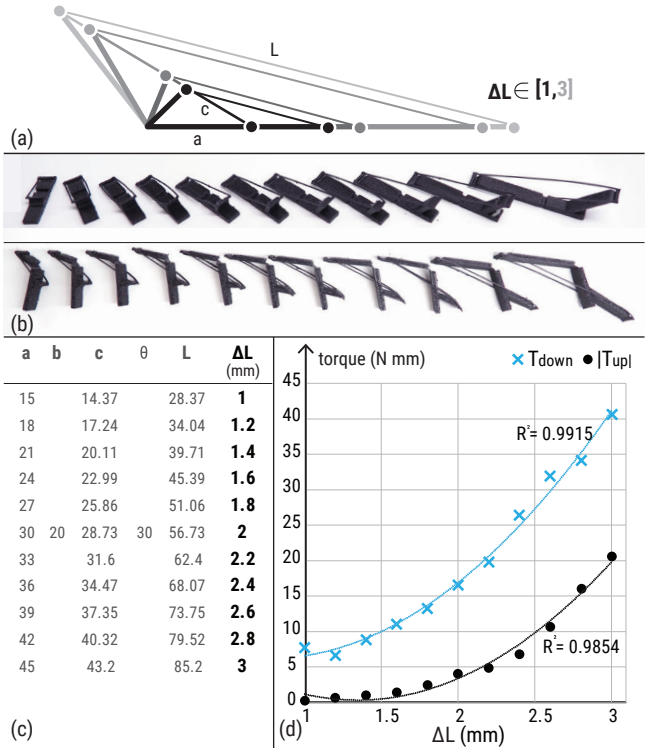

a	b	c	θ	L	ΔL (mm)
15		14.37		28.37	**1**
18		17.24		34.04	**1.2**
21		20.11		39.71	**1.4**
24		22.99		45.39	**1.6**
27		25.86		51.06	**1.8**
30	20	28.73	30	56.73	**2**
33		31.6		62.4	**2.2**
36		34.47		68.07	**2.4**
39		37.35		73.75	**2.6**
42		40.32		79.52	**2.8**
45		43.2		85.2	**3**

Figure 11: (a) Illustrations of variations with different ΔL. (b) We 3D printed the models for force measurement. (c) The results show how ΔL influences the torque.

5.1.5 Varying angle independently from torque. Next, we expanded our experiments and investigated how our design allows for varying the switching angle independently from the switching torques. To do so, we printed 26 new samples. As Figure 12 illustrates, we sampled the parameters for ΔL from 0.8 to 3.2 mm in increments of 0.4 mm, and θ between 15° and 45° in 5° increments. From the total 42 possible parameter combinations, we set the limits for the lengths of a and c with a minimum of 15 mm to ensure bistability, and a maximum of 50 mm, which is larger than half of the average index finger length [32]. We excluded 16 combinations where the lengths of a and c were outside these boundaries.

Our results show that we can customize the switching angle and torque thresholds independently. For example, if we want to increase the switching angle, we can keep the torque the same by decreasing ΔL. Moreover, the results show that our device has a sufficient torque range with up to 43 Nmm to cover the maximum torque of current dynamic splints [25], which is at about 36 Nmm.

5.2 Cyclic Test

To evaluate the durability of our orthosis, we attached a sample to an MG995 servo motor. The switching angle of the test sample was 40°, with a, b, and c are 18 mm. As shown in Figure 13, the

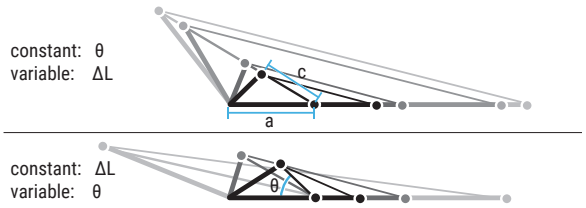

ΔL / θ	0.8		1.2		1.6		2.2		2.8		3.4	
15	13.3	11.52	-		-		-		-		-	
20	14.3	8	23.1	14.6	-		-		-		-	
25	9.9	0	16.5	1.6	23.1	16	35.2	35.2	-		-	
30	6.6	0	6.6	0.6	11	1.4	19.8	4.8	34.1	16	43.4	33.66
35	-		7.7	0	11	1.28	15.4	3.52	22	5.5	29.7	23.46
40	-		-		8.8	0.96	12.1	0.96	18.7	2.42	33	25.5
45	-		-		8.8	0	11	0	14.3	0.44	15.4	16.32

(b) T_{down} $|T_{\text{up}}|$

Figure 12: (a) We varied θ and ΔL independently and (b) measured their maximum switching torques T_{down} and $|T_{\text{up}}|$. The results show how we can tune the switching angle and torques independently.

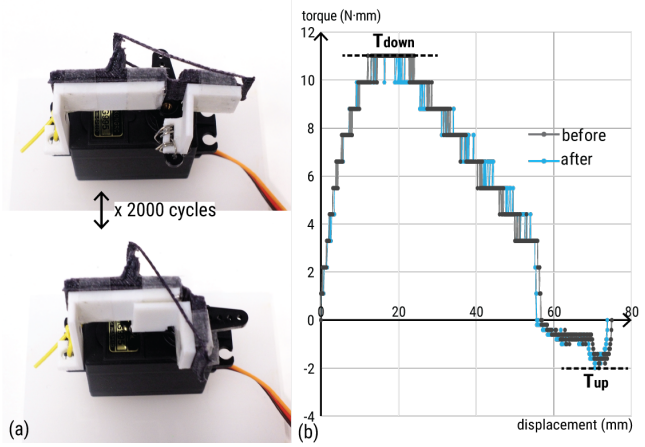

Figure 13: (a) Cyclic test setup. We used a servo motor to drive the orthosis to switch between states. (b) Torque-displacement curves of our tested sample before and after running 2000 cycles.

motor rotated the orthosis to 90° and then returned it to the starting position for more than 2,000 cycles. Each cycle took 5 seconds. We measured the torque before and after the cyclic test. Our results show that switching torques T_{down} and T_{up} remained the same from "before" to "after". To quantify the overall similarity between curves, we calculated the Root Mean Square Error (RMSE) between the torque values at corresponding displacement points, yielding an

RMSE of 0.615 Nmm, significantly smaller than the measurement error margin. Our results confirm that our compliant brace design can withstand frequent switching of states. More extended fatigue tests may be interesting for future product building on our research results.

6 DESIGNING FOR WEARABILITY

After validating our bistable design and its design space, we integrate the mechanism into a wearable form factor. Two key design factors for orthosis wearability are self-alignment and attachment.

6.1 Self-Alignment

When the finger bends, the skin over the joint stretches. As Figure 14 shows, to accommodate this deformation and ensure that our orthosis stays aligned properly with the finger during movement, we cut out space to allow the joint to deform and move the hinge between the rigid bodies of our orthosis towards the middle of the joint accordingly.

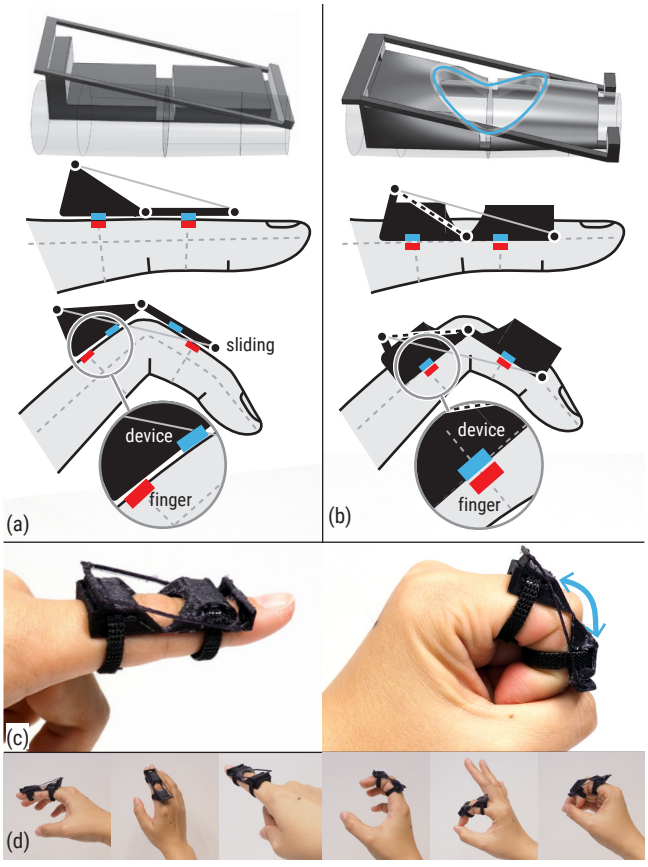

Figure 14: Self-alignment design. (a) To prevent the brace from sliding with the finger when it bends, (b) our design adapts to the finger deformation, which includes space that allows for (c) the deformation of the joint during bending. (d) User can freely move their fingers and perform different gestures with our brace.

6.2 Attachment

We design our attachment (Figure 15a) with a combination of two compliant strips to achieve tight coupling, secure fit, and ease of putting on. First, the attachment must tightly couple the brace to the finger to effectively transmit forces and minimize lift-off during state transitions. To achieve that, we design a less elastic strip near the finger joint to maintain coupling, especially when returning to the stiff state (blue outlined lines illustrated in Figure 15c). The shape of this strip also avoids squeezing the skin when the user attempts to make a fist (Figure 15b). Second, our all-in-one-piece design allows the brace to be easily put on with one hand. Although Velcro straps are commonly used for adjustability, they are difficult to operate single-handedly, as we observe in the next Section. Finally, we incorporate a more elastic strip to balance the need to have a snug fit and accommodate the swollen knuckle, because without a secure fit, sliding can lead to skin irritation, while joint swelling during rehabilitation requires a degree of elasticity for comfort and the ease of putting the brace on through the knuckle. Therefore, the strip with greater elasticity (blue outlined lines illustrated in Figure 15d) is designed to open larger spaces to allow the user to put on the brace and return to its resting shape once in position.

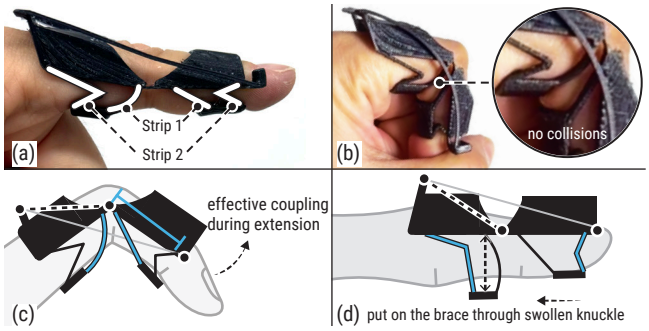

Figure 15: Attachment design. (a) Our brace attachment is composed of two types of strips with different elasticities. Strip 1 (b) allows bending fingers without restrictions, and (c) couples the brace with the finger during movement. (d) Strip 2 supports putting on the brace through the swollen knuckle one-handed, without the need for more adjustment.

7 USER EVALUATION OF WEARABILITY

Our first user study[1] aims to evaluate whether our brace design supports dexterity. We assess (1) how easy it is to put the brace on, (2) whether participants can feel the state transitions of the brace, and (3) how our device influences finger dexterity and daily activities. Since dexterity preservation is our key innovation over static braces, this study focuses on the evaluation of the mobilization mode. We note that this study does not compare against static braces, as they are known to hinder dexterity.

7.1 Procedure

As this is the first user study with this novel device, we refrain from testing with injured patients for safety reasons at this point. The

[1]Carnegie Mellon University IRB #STUDY2022_00000398

findings from healthy participants are valuable for further design decisions, customization, and safe patient testing. We recruited 10 healthy participants from local universities (3 male, 7 female), with an average age of 27 years (SD = 0.82). The study session lasted about an hour, which was compensated with $15. Each participant used the same brace ($\theta = 30°$, $\Delta L = 2$ mm in Figure 10) with velcro strips to adjust it to participants' fingers. We documented participants' verbal feedback and ratings for our study parts.

Figure 16: Our study procedure: (a) Instruction and Wearability, (b) 4 tasks, (c) 30-Minute Free-Use Period

#1: Instruction & Wearability: We first demonstrated to the participants how to put the brace on the index finger of their dominant hand. Then we took it off and asked them to put it on and take it off by themselves. They rated the difficulty of independently putting on the device on a 7-point Likert scale. Next, we asked the participants to slowly bend and extend their braced finger, compare it with the movement of the unbraced hand, and report when they feel the brace switching.

#2: Controlled Dexterous Tasks: Participants performed four short tasks in random order: (1) cutting using scissors, (2) writing, (3) typing a 359-character paragraph, and (4) grasping a bag, a mug with a handle, and a filament spool. Participants were asked to think aloud and rate the difficulty and influence of the brace for each task on a 7-point Likert scale.

#3: 30-Minute Free-Use & Interviews: Participants wore our device for 30 minutes for self-chosen tasks. Afterwards, participants rated task difficulty and the device's influence again using a 7-point Likert scale. We then conducted a semi-structured interview about their experience with the device, including their activities, perceptions, and interactions with the device and any accidental or unsuccessful switches.

7.2 Results

Overall, our results indicate that participants found the brace easy to put on & take off one-handed. They found that the brace did not interfere with the dexterous tasks, with typing being the only exception. We summarized all Likert-scale ratings in Figure 17 and will discuss detailed results in the following.

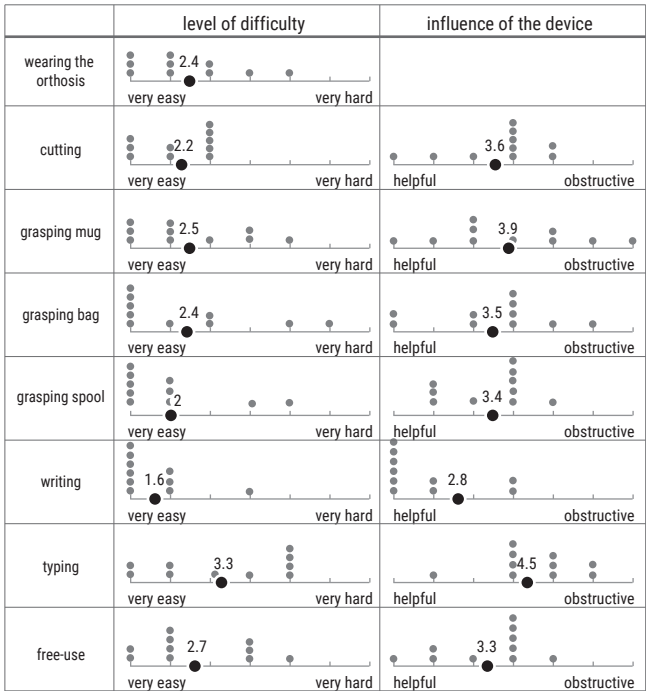

Figure 17: Participants' ratings of the difficulty and impact of our devices on specific tasks and daily activities. The numbers on the scale are the average ratings across the participants.

Ease of wearing one-handed . All participants were able to put the device on and off independently. The difficulty mainly depends on whether they need to adjust the Velcro strap, which is hard with one hand. P2 noted that the design provided helpful alignment as the hole in the middle was "*a visual affordance to align the joint.*

I can even close my eyes and do it". This result validated the later development of our attachment structure mentioned in Section 6.2.

Perceived state switching. Most of the participants (8/10) could feel and predict when the device was about to switch states. They described the sensation as "*the resistive force gradually increases*" (P1), followed by "*a sudden point*" (P4). After switching, the participants noted reduced resistance (P4, P7). Several participants also mentioned that extending the finger was easier than bending it (P1, P2, P7, P8, P9). They also observed differences in motion patterns compared to their unbraced hand. All participants noticed that the braced finger started "*moving slower*" (P1) while "*accelerated at some points*" (P7).

Finger dexterity in daily activities. All participants successfully completed the four dexterous tasks. As the ratings in Figure 17 show, tasks involving stable grip (writing, grasping small and large objects, using scissors) were rated easiest, and participants generally reported that the brace did not obstruct their tasks. However, tasks requiring rapid finger extension and flexion, such as typing with the braced finger, were more challenging and needed more practice (P1, P10). Some participants also mentioned challenges in placing the braced finger together with other fingers through narrow spaces like scissor handles (P3, P4, P9).

During free use, participants reported ease during social interactions (P1), photography (P5, P6), using painting spray (P2), and tool assembly (P2, P10). More difficult tasks included peeling bananas (P4) and operating precise tools like Vernier calipers (P7).

Dual functionality. All participants reported that the device kept their fingers straightened more often during rest ("*When relaxed, it always gets it straight*" (P7)), such as, during social interactions (P1), which is encouraging for supporting the immobilization schedule. For the mobilization routine, P10 mentioned that they should "*bend it purposefully (to involve the finger in daily activities)*". In terms of the range of motion, most participants were able to make a full fist, while three could not fully touch their palm with the braced finger tip (P6, P8, P10), restricted by the Velcro strips. Accidental switches were rare and mainly mentioned during typing (P2, P4, P10).

Comfort and satisfaction. Most participants found the device very comfortable, lightweight, and natural to use. "*After 5 minutes, I got used to it and barely felt it.*" (P2). Participants also found the device more resilient than expected (P1, P2). Reported issues included discomfort from improper fit (P1, P6), irritation from Velcro straps, and occasional slippage due to sweat (P2, P8). Participants hoped to have customized sizing (P2) and switching angle (P7, P8), like "*a smaller degree of bending would help with typing.*" (P8). This highlights the importance of customization in orthosis design.

Interestingly, P9 hoped to get one for their knee, "*I like it a lot. I want one for my leg, as I have a knee problem and want to keep it straight.*" P10 was interested in having braces on all the fingers, saying that "*for the tasks that I feel helpful like writing and grasping, the experience will be enhanced if I use it on all the fingers.*"

8 CUSTOMIZATION PIPELINE

We develop a customization tool for therapists and physicians who prescribe braces for patients. Physicians can customize the bistable finger orthosis by entering the patient's finger measurement data. Our computational design tool optimizes personalized orthosis models. Users can then download the corresponding '.STL' file for 3D printing.

8.1 System Overview

Our customization tool, shown in Figure 18, consists of three primary components: (1) User inputs: a web-based interface that collects measurement data, including the patient's finger dimensions, extension angle, and strengths. Users can also select the desired device strength levels. (2) Parameter optimization: When the user clicks "Generate", a simulation-based optimizer processes the input finger angle and strengths, and computes the optimal brace geometric parameters. (3) Parametric modeling system: generates the brace model based on the optimized parameters and finger dimensions. The user can then download the final result.

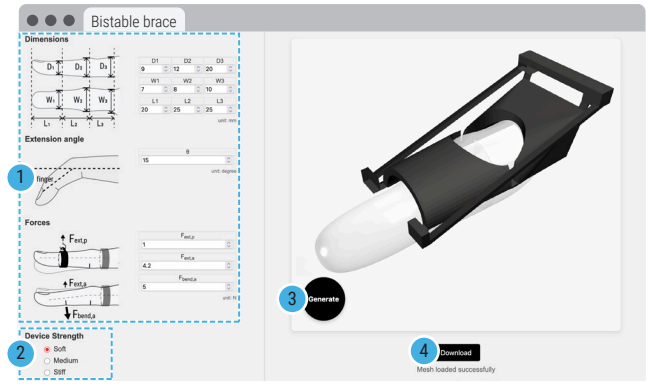

Figure 18: Our user interface that supports the workflow of ① user input of finger measurement results, ② selecting device strengths, ③ generating the brace model and preview it on the finger, and ④ downloading the brace model.

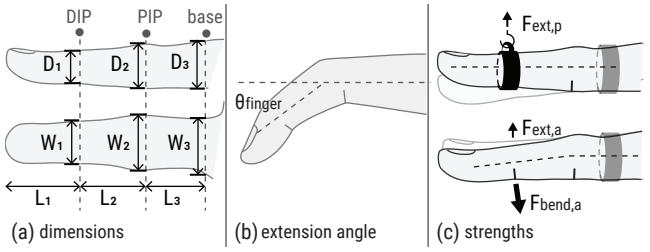

Figure 19: The finger measurement data include (a) finger dimensions, (b) extension angle, and (c) strengths

8.2 Input: Finger Measurement

Three types of finger measurement data are needed as input, as illustrated in Figure 19. Measurements can be taken with common tools, such as a ruler or caliper for dimensions, a goniometer or protractor for extension angle, and a force gauge for strength (e.g., a simple spring scale).

The *finger dimensions* (Figure 19a) define the finger mesh and the brace size. These include the widths (W_1, W_2, W_3) and depths (D_1, D_2, D_3) of the distal interphalangeal (DIP) joint, PIP joints, and the finger base, as well as the lengths (L_1, L_2, L_3) of the phalanx segments between joints.

The *extension angle* measurement (Figure 19b) is only necessary for patients with extensor lag, and is taken when the user extends the finger as far as possible without pain. For patients with a full active range of motion, such as our case study participant (next Section), we define the switching angle as 20–25° to allow distinct switching perception and prevent accidental switching.

The *finger strengths* (Figure 19c) define the target torque thresholds. The first is finger stiffness, or the passive extension force ($F_{\text{ext,p}}$). To measure it, the patient relaxes the joint in an extended position, and the clinician pulls the gauge perpendicularly until the joint is fully or comfortably extended without the finger applying active effort. Secondly, active bending force ($F_{\text{bend,a}}$) can be obtained with the clinician holding the gauge steady while the patient actively bends the joint as strongly as comfortably possible. Thirdly, active extension force ($F_{\text{ext,a}}$) is measured by the patient flipping the hand and actively extending the joint with the maximum comfortable effort, with the clinician holding the gauge steady. When taking measurements, the force gauge is always connected to the DIP joint, and the resulting torques are calculated by multiplying the measured forces by L_2, the distance between the DIP and PIP joints.

8.3 Simulation-Driven Optimization

The user's extension angle and strengths define the switching angle and the ranges of the torque thresholds of the target brace geometry of our simulation-based optimizer, as Figure 20 shows.

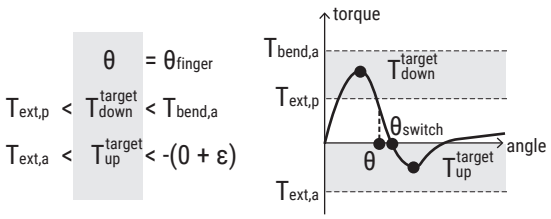

Figure 20: The target values of our optimization. $T_{\text{bend, a}}$, $T_{\text{ext, p}}$, $T_{\text{ext, a}}$, and θ_{finger} represent finger metrics: active bending torque, passive extension torque, active extension torque, and maximum extension angle. $T_{\text{down}}^{\text{target}}$, $T_{\text{up}}^{\text{target}}$ and θ are the target device properties for our optimizer.

First, $\theta = \theta_{\text{finger}}$, the user's maximum extension angle. θ is inherently smaller than the actual switching angle θ_{switch} (Figure 6a), which is the point at which the orthosis switches states. As shown in the torque–displacement curve (Figure 20), θ_{switch} is labeled at the first zero crossing of the curve. By assigning $\theta = \theta_{\text{finger}}$, users are able to pass the switching angle θ_{switch} to trigger the upward snap during finger extension. This relationship ($\theta < \theta_{\text{switch}}$) results from hinge stiffness, which introduces an upward restoring force as the hinge bends away from its fabricated shape. We note that this force not only shifts the switching point but also reduces the magnitude of the extension torque threshold, making $|T_{\text{up}}|$ smaller than T_{down}.

Second, the downward switching torque $T_{\text{down}}^{\text{target}}$ must be greater than the finger's passive extension force ($T_{\text{ext,p}}$) to keep the finger straight and avoid accidental switch, yet smaller than the user's active bending torque ($T_{\text{bend,a}}$) to allow intentional flexion. Note that for the two indications we focus on, $T_{\text{bend,a}}$ is typically greater than $T_{\text{ext,p}}$, which is a key condition for our device and optimization function.

Lastly, to ensure bistability, the upward switching torque $T_{\text{up}}^{\text{target}}$ must be negative, and its magnitude should be smaller than the user's active extension torque ($T_{\text{ext,a}}$) to allow the user to trigger the return to the extended state.

8.3.1 Simulation. Our brace geometry optimizer is supported by our physics-based simulator. We implemented a MuJoCo [46] model of our parametric orthosis attached to a finger and simulated the torque exerted by the finger during movement. This process computes the torque-angle profile for a given geometry.

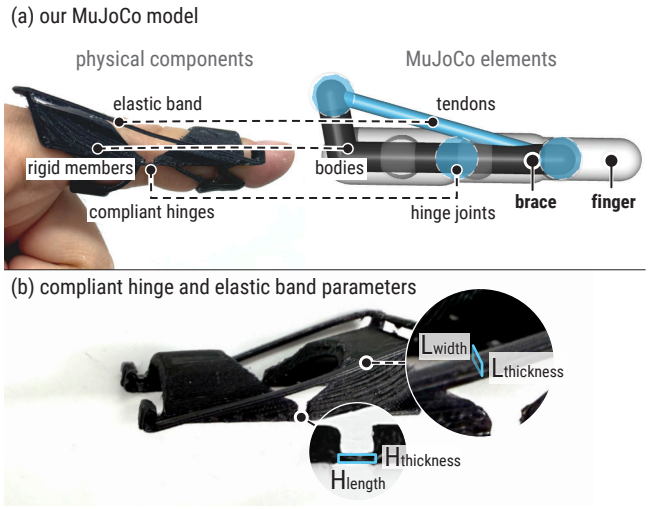

Figure 21: 3D Representation of the (a) MuJoCo model, where the compliant hinge and elastic band properties are defined by (b) their parameters.

Modeling. We model the finger and brace's rigid links, compliant hinges, and elastic band with MuJoCo built-in elements, as Figure 21a shows. The finger is modeled as rigid bodies connected by hinge joints.

The brace's rigid members are modeled as bodies as well. Three compliant hinges of the orthosis are modeled as hinge joints, with the joints' stiffness and damping scaling with the brace's hinge geometry $H_{\text{k}} = \frac{H_{\text{thickness}}^3}{H_{\text{length}}}$ (Figure 21b), based on the pseudo-rigid-body model [54]. While hinge width also affects stiffness, we keep it constant at 2 mm to maintain structural strength while minimizing the overall brace profile. To simplify the model and reduce the number of parameters, all three hinges use the same dimensions. We model the elastic band as the combination of two tendon elements: one for bending and one for extension. The bending tendon behaves

like a hinge joint, with properties that change based on elastic band geometry. The extension tendon stiffness scales with cross-sectional area [11] ($L_A = L_{thickness} \cdot L_{width}$, as Figure 21b shows), and its rest lengths are determined by a, c, and θ.

Simulation process. To simulate the torques during the finger bending process, we gradually increment the finger joint angle $\Delta\alpha$, compute the kinematics and dynamics of the system, and record the torque through the MuJoCo sensor attached to the PIP joint (Figure 22). To capture the nonlinear material behavior in large deformations of the hinge connecting two rigid members, an additional actuator is attached to the corresponding hinge joint and exerts resistive torques proportional to $\Delta\alpha^3$ at each step, determined by beam theory and empirical testing. From the output torque-angle curve, we can extract the simulated device torque thresholds T_{down} and T_{up}.

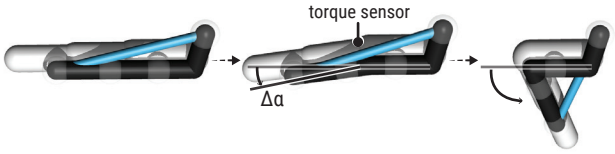

Figure 22: The simulation process by incrementing $\Delta\alpha$ and measuring the finger torque through the torque sensor.

Material properties tuning. To match the simulation results to actual behavior with our material (PCTPE) and 3D printing settings, we tuned the material properties, including the coefficients of the stiffness and damping of the hinge joints and tendons, and the nonlinear stiffness coefficients of the hinge joint under large bending.

We printed five samples with varying geometric parameters and collected their torque data experimentally. We then employed a differential evolution algorithm [43] to fine-tune these coefficients by minimizing the difference between the simulated and measured values of T_{down} and T_{up} (Figure 23). The resulting root mean square errors (RMSE) were 5.10 N·mm for T_{down} and 3.25 N·mm for T_{up}.

To estimate the inherent fabrication and measurement variability, we also printed the same model twice and measured the torque profiles. The deviation between the two prints was 2 N·mm for T_{down} and 3.2 N·mm for T_{up}, suggesting that a portion of the observed error stems from the measurement and the fabrication process.

Features. As identified in Section 5, the geometric parameter that has the greatest impact on torques is ΔL. In addition, the hinge geometry H_k and elastic band geometry L_A influence the hinge joints and tendons' stiffness and damping.

To understand how each key parameter impacts the simulation result, we simulated three sets of models, each including 10 data points varying a single parameter while holding others constant. As shown in Figure 24, increasing the tendon offset ΔL or the elastic band cross-sectional area L_A leads to higher absolute values of both T_{down} and T_{up}. When increasing the hinge geometry ratio H_k, the upward torque decreases in magnitude, as expected.

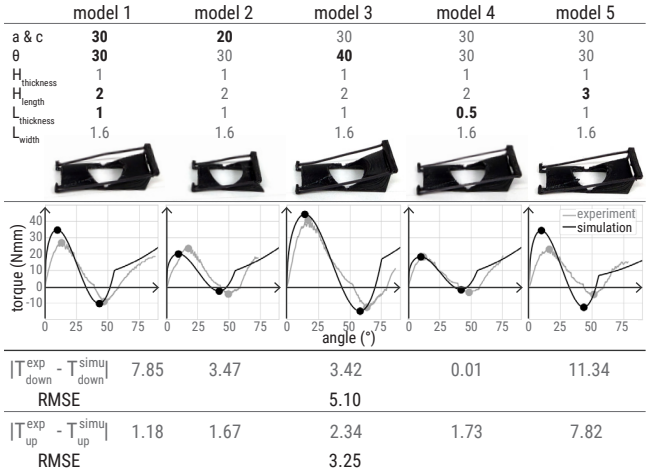

Figure 23: We printed five test samples to fit our simulated material properties with the experimental data. For each model, we reported the deviation of T_{down} and T_{up} between the fitted simulation and the corresponding experimental measurements. We also reported the RMSE for T_{down} and T_{up} across all samples.

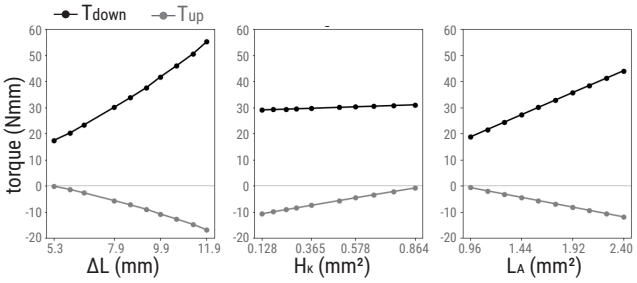

Figure 24: Impacts of key parameters ΔL, H_k and L_A to simulated T_{down} and T_{up}.

8.3.2 Optimization. With our simulation, we can optimize the geometric parameters that yield the desired T_{down} and T_{up}. To do that, we employed the differential evolution algorithm [43]. Our optimization objective is as below.

$$\theta = \theta_{finger} \tag{1}$$

$$\min_{\Delta L, L_A, H_k} \left(T_{down} - T_{down}^{target}\right)^2 + \left(T_{up} - T_{up}^{target}\right)^2 \tag{2}$$

The bounds of the decisive variables ΔL, L_A, and H_k are determined based on the geometric parameters from which they are derived. Specifically, ΔL is derived from a and c, which are bounded between 15 – 50 mm according to our technical evaluation. The bounds for H_k and L_A are constrained by the thickness and width or length to ensure printability and preserve elasticity.

8.3.3 Evaluation. To evaluate the performance of our optimization, we randomly selected four sets of target values T_{down}^{target}, T_{up}^{target} and θ_{finger}, then let our optimizer generate corresponding models, 3D printed these brace models and compared their actual T_{down} and

T_{up} with the target values. The results are shown in Figure 25. As expected, $\theta_{finger} < \theta_{switch}$ holds for all samples. Across all models, the RMSE was 12.54 N·mm for downward torque and 6.36 N·mm for upward torque, with actual torque values tending to be higher than the targets.

The current optimizer error is because the torques are highly sensitive to hinge joint and tendon stiffness, which is determined by their thickness, width, and length. The optimizer can produce hinges and tendons with small differences in dimensions (1e-7), which cannot be accurately reproduced by our 3D printer, as we set the layer height to 0.3 mm for robust printing using our semi-soft PCTPE filament. However, this is a technical limitation introduced by our printers and may be mitigated using high(er)-resolution printers or adjusting the optimizer to account for this error. We have done the latter and accommodated the error in our optimization routine. Also, since current dynamic orthoses are not personalized or adapted to patients, which is an issue for patients' tolerance (as discussed in Section 3.4), there is no RMSE baseline that exists for comparison. Our computational design tool that customizes for patients' strength addresses this gap.

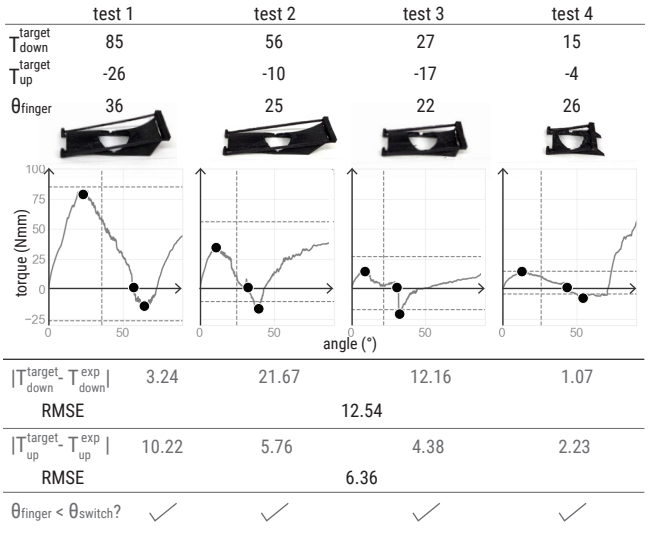

Figure 25: Comparison of the actual torques and switching angle of generated braces and the target torques and angle.

To accommodate the optimizer error and produce a brace with appropriate switching thresholds for the user, we establish conservative ranges of target torque thresholds with safety margins, as Figure 26 illustrates. Specifically, for downward torque, T^{target}_{down} should be defined within the range ($T_{ext,p}$ + 12.54, $T_{bend,a}$ − 12.54) N·mm, while the upward torque T^{target}_{up} is set within (-($T_{ext,a}$ − 6.36), -6.36) N·mm, by applying error margins of ±12.54 N·mm and ±6.36 N·mm respectively. To allow users to toggle between different brace strengths, in our system, we set T^{target}_{down} to 70%, 50%, and 30% of the allowable downward torque range for the stiff, medium, and soft versions, respectively. We set T^{target}_{up} to 50% of the upward torque range.

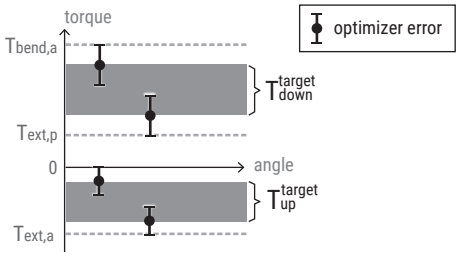

Figure 26: The ranges of T^{target}_{down} and T^{target}_{up} are defined based on the optimizer error.

8.4 Output: Parametric Modeling

Finally, our parametric modeling generates ready-to-print orthosis models that conform to the patient's specific finger dimensions while implementing the optimized parameters. We implemented it using the Blender Python API (bpy)[2], and Constructive Solid Geometry (CSG) techniques.

To avoid pressure on potentially swollen joints, we modeled the finger by performing radius interpolation along the finger axis to capture dimensional variations at different longitudinal positions. The brace is positioned by aligning the hinge between the rigid members with the center of the PIP joint. We also adjust the device width based on the maximum width of the finger. After modeling the brace, we apply Boolean operations to create clearances between the brace and the finger.

9 CASE STUDY

After evaluating the intended functionality of our brace with healthy participants, we set out to understand how well patients tolerate it. Our main goal was to gather initial data about comfort and usability on an injured finger. Aligned with medical device development protocols for early-stage evaluation, e.g., single-case experimental design approach [23], we recruited one patient with an extensor tendon injury who consented to participate in our case study voluntarily. They cleared the use of our brace with their physician, who supervised this study, and were compensated with $100 for their 2-week participation (Carnegie Mellon University's IRB #STUDY2024_00000267).

9.1 Participant

The participant was a 47-year-old woman with an extensor tendon injury on her left ring finger, following a PIP joint dislocation (Figure 27a). She started our study about one month after her injury, when her doctor advised her to start mobilization. At that time, her affected finger had a full range of motion, but was swollen, and trying to make a fist was painful. This pain affects her daily activities that require her to bend her finger. She couldn't grip a pen, glass, or pillow, because that hurts. As a blogger, "*it hurts to type–because I'm not paying attention, I'm just in the groove of typing and using that finger*".

According to her physician, her knuckle swelling and soreness could last about 4-6 months. She was advised the rehabilitation

[2]https://docs.blender.org/api/current/index.html

routine of wearing a brace to keep the finger straight for a few hours, and to remove their brace and exercise the finger periodically, which is the rehabilitation scenario described in Section 3.2. She checked in with her doctor about every 2 weeks.

Before the study, she had been using a Rolyan Baseball Splint (Figure 27b), a static splint that immobilizes all finger joints, for 6-8 hours per day for a month. While the splint provided protection, she preferred not wearing any brace when she felt there was no risk of aggravating the injury. During active hand use, however, she relied on the splint, even though she noted it interfered with most of her daily activities, including house cleaning, laundry, yoga, dog walking, and typing for her blogs.

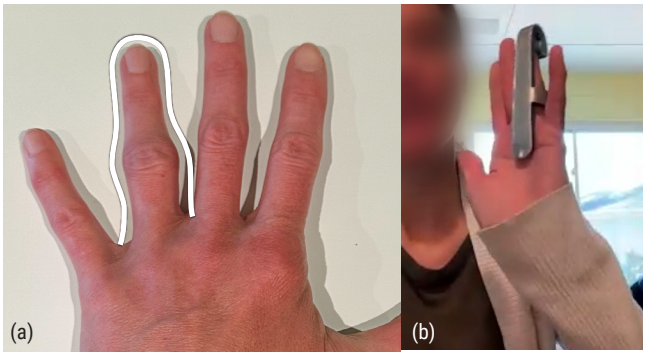

Figure 27: (a) The injured finger of the participant. (b) The previous splint she was using before the study.

9.2 Fitting the Brace

After introducing the participant to our brace and study, we took measurements of her finger dimensions and strengths (Figure 28a) through the process as described in Section 8.2.

We customized 3 braces for our participant with different strengths (Figure 28b). We measured three braces before mailing them to the participants, all of which fit within the participant's finger measurement range.

On a video call, she tried all three braces on. Brace 1 (medium strength) fitted her affected finger best. Brace 3 was tighter (low strength), but still comfortable. She mentioned that movement using the 2nd brace took more effort, which is the stiffest brace. As Figure 28c shows, wearing our brace allowed the participant to extend her finger completely and flex it a bit without pain, although attempting to bend approximately 80° still caused discomfort regardless of whether the brace was worn.

9.3 Comparison with Her Previous Brace

On the same video call and with brace 1 properly fitted, we asked the participant to compare it with her previous splint by performing tasks that reflect her daily routine. She selected writing, grasping a cup and a pillow, using a broom, and typing as her tasks. After each task, she rated the difficulty of the task and how each brace influenced her performance.

As the ratings in Figure 29 show, our brace made all five tasks easier. As expected, the long static brace covering her palm partially

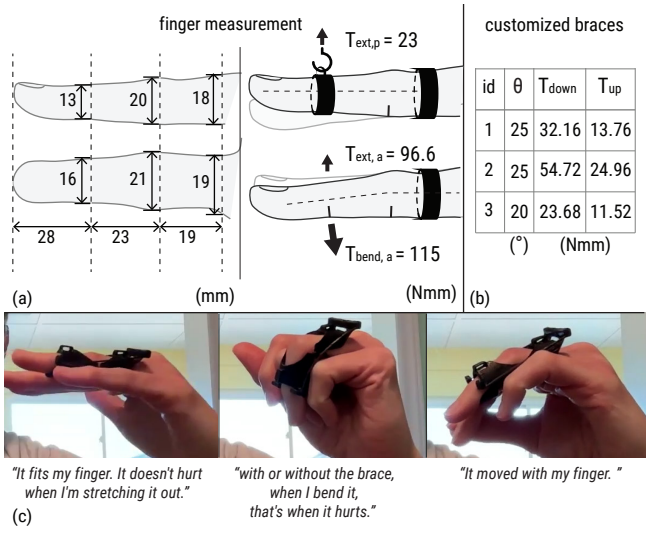

Figure 28: (a) Participant finger measurement data. (b) We customized three braces for the participant with different switching angles and torques. (c) The participant wore our brace.

hinders her daily activities a lot. With our brace, she can easily complete all the tasks. Despite her dominant hand being injured, writing was manageable with our brace. While grasping the pillow, she mentioned: "*I wouldn't have done it–it would have hurt without the device. And if I had the other splint on, the metal splint, I wouldn't have been able to pick it up like that because it would have kept my finger straight. This is allowing me to move my finger back and forth, which is very helpful.*"

9.4 Daily Experience with Our Brace

The participant kept and used the brace for 15 days, with 13 days of diary input. During the documented 13 days, the participant wore our brace between 3 and 7 hours, averaging 5.3 hours per day. She wore it during active hand use and wore no brace otherwise, i.e., during idle times. "*When I'm really just hanging out and not doing anything, I won't wear a brace... not really moving my hand.*"

During the study period, the participant found wearing our brace made all her daily activities easier, getting dressed, buttoning clothes, holding a book for reading, picking up the phone, household chores (cleaning, laundry), lifting grocery bags, dog walking, doing yoga, etc. Opening jars is still difficult with a knuckle injury. "*I did some cleaning, dishes & dog walking so it helped to keep my finger in a good & comfortable position. I like that the brace allows me to bend my finger safely while I'm busy with a task, when I'm not actually trying to bend it on purpose.*" Aligned with our wearability study results, their hand movement seems to get more natural, and they don't pay much attention to the brace because they don't feel it.

Occasional switching occurred, but only during highly active hand use. "*The brace would switch sometimes, but only while I was using my hand more actively during chores, etc. The brace stayed in position for most of the time I was wearing it.*"

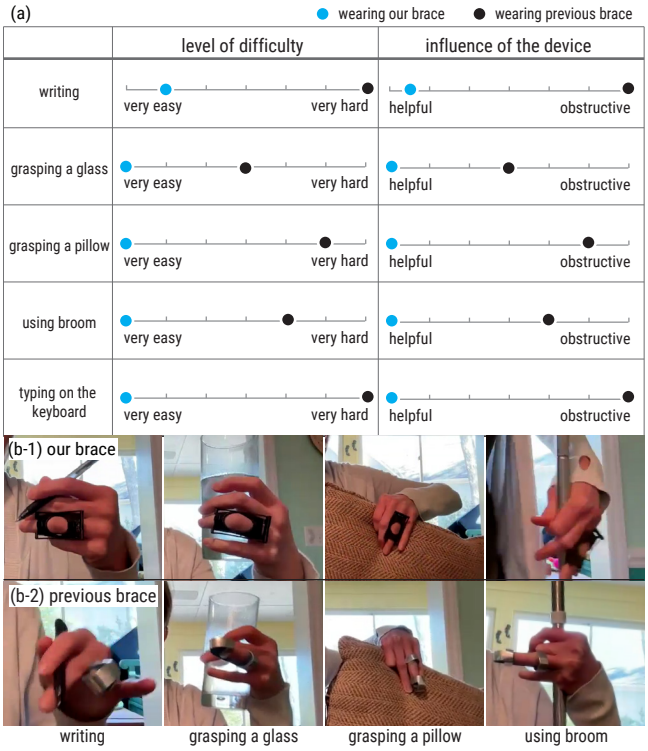

Figure 29: (a) The participant's ratings of the difficulty and impact on specific daily tasks of (b-1) wearing our brace and (b-2) their previous braces. We didn't take the screenshots of the typing process as it was out of view.

The participant switched to using different strengths and tightness of our braces based on their activities. "*If I want to feel it move (during tasks involving hands), I will switch to a little tighter one. When I'm sleeping, I usually like a loose one.*" The participant liked wearing our brace 1 or 2 during sleep, compared to her static one. "*The other day I decided I'm gonna put the metal one back on and sleep... when I woke up... my finger felt very stiff. [...] When I sleep with the other ones from you, I feel better because my finger's actually able to bend while I'm sleeping.*"

9.5 Tendon Injury and PIP Joint Rehabilitation

After the 2-week study, the participant met with her physician, who confirmed positive progress on her finger healing. "*He was impressed with my improvement & ability to almost make a fist. He said, continue staying on that path. He suggests that I continue to use the braces when I'm using my hands. He said it's my choice to use them while sleeping, so I'll probably put them on before bed a few times a week.*"

We further followed up with the participant and her physician about the safety of using the brace. None of them saw any safety issues. The participant said: "*I never felt unsafe using the brace.*" On the contrary, the physician said our brace allows the patient to move *more* safely because it adds lateral support that would be missing otherwise. Moreover, they expressed that this brace is beneficial in that it allows them to prescribe one brace instead of two (first a static, then a dynamic brace) and that physicians can advise patients with regular check-ins on how to use it, e.g., first in static mode, then start using it in dynamic mode depending on their healing.

While we do not intend to evaluate and generalize any result about efficacy, but rather comfort in this study, we are pleased to hear this feedback, encouraging larger and longer-term studies in the future.

9.6 Learnings and Future Work

While the brace fit overall well and the strength and switching thresholds seemed appropriate, the tightness of the attachments can be refined. Overall, the participant liked the flexibility when wearing our brace but noted that it occasionally slid with her finger. Other versions of the brace "*too tight*" around her injured knuckle, and left indentations after longer use. She guessed the reason was that her swollen knuckle size changes daily, "I think the accuracy of fit depends on multiple factors since my hands contract & swell throughout the day, depending on my activities."

Therefore, we found a good fit would be loose enough when putting the brace on and snug once positioned. We plan to research swelling and leave enough tolerance around the joint, while keeping the attachments tight enough to prevent sliding. Additionally, we plan to investigate padding structures that can compress to compensate for swelling.

10 LIMITATIONS

Overall, both the wearability study and the case study results demonstrate that our novel bistable brace design is promising for supporting rehabilitation routines involving intermittent immobilization and mobilization. We acknowledge limitations in our research prototypes, which also suggest interesting directions for future research and development.

Rigidity. The PCTPE filament used in our prototypes is well-suited for wearable applications due to its high elongation at break and moderate elasticity. However, the brace still exhibits rigid edges, which may reduce comfort during prolonged wear or under pressure. Future work could explore incorporating hyperelastic structures or softer padding layers to provide additional damping and minimize discomfort where the brace contacts the skin.

Fit. Our case study highlighted challenges in achieving a secure yet comfortable attachment and custom fit, particularly around the knuckle where swelling and soft tissue deformation are common and changing during the rehabilitation. To better accommodate these anatomical variations, we are interested in enhancing the customization pipeline by incorporating buffer zones or by locally expanding the finger model geometry (e.g., around the PIP joint) before subtracting the brace mesh. This could reduce the risk of pressure points or indentations during extended use.

Form factor. As mentioned by participants in our wearability study, users have challenges putting the braced finger into a tighter space, such as smaller scissor handles. To make our device lower profile, as discussed in our technical evaluation, materials that are more rigid, such as Polycarbonate (PC) and Nylon (PA), can

reduce the amount of ΔL to reach the same switching torque. In this way, it's promising to change the device force profiles with fewer increases in rigid link lengths (a and c).

Fabrication. Our current implementation is optimized for FDM printing with post-processing (e.g., support removal and surface smoothing). To support broader adoption and a more user-friendly fabrication process, we are investigating how to tune our design tool for selective laser sintering (SLS) materials, as SLS printing offers improved surface finish and precision. Additionally, since many 3D printing services offer high-quality SLS printing, this can democratize the process, such that patients can design their brace using our computational design tool and order their custom brace directly.

11 CONCLUSION & FUTURE WORK

We presented a novel orthotic device design that facilitates rehabilitation and dexterity. To achieve this, we designed a bistable mechanism with one stiff state, keeping the joint immobilized for rehabilitation. When users intentionally bend their joints, the brace switches into its flexible state, allowing users to go about their daily tasks. This dual-functional device remains unpowered, unactuated, and simple to use, supporting patients during their rehabilitation process. Our technical evaluation demonstrates that our design enables personalization for different users' finger dimensions and rehabilitation needs. Our wearability study confirms that our design effectively supports dexterity through modes. Finally, our case study provides evidence that our design holds significant promise for joint rehabilitation applications.

We see this as just the beginning, which opens the door to exploring passive yet multifunctional mechanisms and patient-centered customization in real-world rehabilitation and healthcare contexts. In the future, we plan to conduct further studies involving a larger number of patients to better understand how our brace supports the full rehabilitation journey. In addition, we are excited to explore how our bistable design can be applied to other hand-related conditions and rehabilitation scenarios beyond extensor tendon injuries, such as flexor lag, finger contracture, and conditions affecting the distal interphalangeal (DIP) joints.

Given its simple design and customizable strength, our device can be scaled up. We believe that our brace design can be adapted to other limb joints, such as knee extensor lag, or the wrist (e.g., in post-operative stabilization or tendon rehabilitation). This shows a roadmap and potential broader application space of such bistable braces. This is a broader space with many open research questions and opportunities.

Acknowledgments

The work in this paper was supported in part by the National Science Foundation under Award No. IIS-2443190.

We thank Jodi Seffchick, Jacqueline Voegler, and Anthoney M Lovat from University of Pittsburgh Medical Center for insightful discussions about clinical practice. We thank our study participant, who generously shared her time and experience with us. We thank Yue Jiang for the insightful discussions; Wesley Deng, Yunzhi Li, and Jianzhe Gu for help with paper proofreading; Xiaolei Lu, Wesley Deng, Hongyu Mao, and Yi-Hao Peng for support.

References

[1] Benjamin WK Ang and Chen-Hua Yeow. 2017. Print-it-Yourself (PIY) glove: A fully 3D printed soft robotic hand rehabilitative and assistive exoskeleton for stroke patients. In *2017 IEEE/RSJ International Conference on Intelligent Robots and Systems (IROS)*. IEEE, 1219–1223.

[2] Brian G. Beutel, Kenneth S. Gutowski, and Ranjan Marappa-Ganeshan. 2025. *Hand Extensor Tendon Lacerations*. StatPearls Publishing, Treasure Island (FL). https://www.ncbi.nlm.nih.gov/books/NBK554431/ [Updated 2024 Oct 5].

[3] Catherine Bracks. 2007. Low profile extension splint for active extensor lag of the proximal interphalangeal joint. *Journal of Hand Therapy* 20, 3 (2007), 274–276.

[4] Tian Chen, Osama R Bilal, Kristina Shea, and Chiara Daraio. 2018. Harnessing bistability for directional propulsion of soft, untethered robots. *Proceedings of the National Academy of Sciences* 115, 22 (2018), 5698–5702.

[5] Yinding Chi, Yanbin Li, Yao Zhao, Yaoye Hong, Yichao Tang, and Jie Yin. 2022. Bistable and multistable actuators for soft robots: Structures, materials, and functionalities. *Advanced Materials* 34, 19 (2022), 2110384.

[6] Shrikant J Chinchalkar and Bing Siang Gan. 2003. Management of proximal interphalangeal joint fractures and dislocations. *Journal of Hand Therapy* 16, 2 (2003), 117–128.

[7] Judy C Colditz. 1996. Principles of splinting and splint prescription. *Surgery of the hand and upper extremity* 2 (1996), 2389–410.

[8] Johanna P De Jong, Jesse T Nguyen, Anne JM Sonnema, Emily C Nguyen, Peter C Amadio, and Steven L Moran. 2014. The incidence of acute traumatic tendon injuries in the hand and wrist: a 10-year population-based study. *Clinics in orthopedic surgery* 6, 2 (2014), 196.

[9] Donatella Dragone, Luigi Randazzini, Alessia Capace, Francesca Nesci, Carlo Cosentino, Francesco Amato, Elena De Momi, Roberto Colao, Lorenzo Masia, and Alessio Merola. 2022. Design, computational modelling and experimental characterization of bistable hybrid soft actuators for a controllable-compliance joint of an exoskeleton rehabilitation robot. In *Actuators*, Vol. 11. MDPI, 32.

[10] Jakob A Faber, Janav P Udani, Katherine S Riley, André R Studart, and Andres F Arrieta. 2020. Dome-Patterned Metamaterial Sheets. *Advanced Science* 7, 22 (2020), 2001955.

[11] James M. Gere and Barry J. Goodno. 2012. *Mechanics of Materials* (8 ed.). Cengage Learning, Boston, MA.

[12] Michelle Griffin, Sandip Hindocha, D Jordan, Mahmoud Saleh, and Wasim Khan. 2012. Management of extensor tendon injuries. *The Open Orthopaedics Journal* 6 (2012), 36.

[13] Xiaochi Gu, Yifei Zhang, Weize Sun, Yuanzhe Bian, Dao Zhou, and Per Ola Kristensson. 2016. Dexmo: An inexpensive and lightweight mechanical exoskeleton for motion capture and force feedback in VR. In *Proceedings of the 2016 CHI Conference on Human Factors in Computing Systems*. 1991–1995.

[14] Takeru Hashimoto, Shigeo Yoshida, and Takuji Narumi. 2023. SomatoShift: A Wearable Haptic Display for Somatomotor Reconfiguration via Modifying Acceleration of Body Movement. In *ACM SIGGRAPH 2023 Emerging Technologies* (Los Angeles, CA, USA) *(SIGGRAPH '23)*. Association for Computing Machinery, New York, NY, USA, Article 17, 2 pages. https://doi.org/10.1145/3588037.3595390

[15] Megan Hofmann, Jeffrey Harris, Scott E Hudson, and Jennifer Mankoff. 2016. Helping hands: Requirements for a prototyping methodology for upper-limb prosthetics users. In *Proceedings of the 2016 CHI conference on human factors in computing systems*. 1769–1780.

[16] Megan Hofmann, Kristin Williams, Toni Kaplan, Stephanie Valencia, Gabriella Hann, Scott E Hudson, Jennifer Mankoff, and Patrick Carrington. 2019. " Occupational Therapy is Making" Clinical Rapid Prototyping and Digital Fabrication. In *Proceedings of the 2019 CHI conference on human factors in computing systems*. 1–13.

[17] Amy Hurst and Jasmine Tobias. 2011. Empowering individuals with do-it-yourself assistive technology. In *The proceedings of the 13th international ACM SIGACCESS conference on Computers and accessibility*. 11–18.

[18] Alexandra Ion, Ludwig Wall, Robert Kovacs, and Patrick Baudisch. 2017. Digital Mechanical Metamaterials. In *Proceedings of the 2017 CHI Conference on Human Factors in Computing Systems* (Denver, Colorado, USA) *(CHI '17)*. Association for Computing Machinery, New York, NY, USA, 977–988. https://doi.org/10.1145/3025453.3025624

[19] Yu Jiang, Shobhit Aggarwal, Zhipeng Li, Yuanchun Shi, and Alexandra Ion. 2023. Reprogrammable digital metamaterials for interactive devices. In *Proceedings of the 36th Annual ACM Symposium on User Interface Software and Technology*. 1–15.

[20] Vicki Kaskutas and Rhonda Powell. 2013. The impact of flexor tendon rehabilitation restrictions on individuals' independence with daily activities: implications for hand therapists. *Journal of Hand Therapy* 26, 1 (2013), 22–29.

[21] Aisling Kelliher, Setor Zilevu, Thanassis Rikakis, Tamim Ahmed, Yen Truong, and Steven L Wolf. 2020. Towards standardized processes for physical therapists to quantify patient rehabilitation. In *Proceedings of the 2020 CHI Conference on Human Factors in Computing Systems*. 1–13.

[22] Jin Hee Kim, Joan Stilling, Michael O'Dell, and Cindy Hsin-Liu Kao. 2023. Knitdema: robotic textile as personalized edema mobilization device. In *Proceedings*

of the 2023 CHI Conference on Human Factors in Computing Systems. 1–19.

[23] Agata Krasny-Pacini and Jonathan Evans. 2018. Single-case experimental designs to assess intervention effectiveness in rehabilitation: A practical guide. *Annals of physical and rehabilitation medicine* 61, 3 (2018), 164–179.

[24] Mikko Kytö, Laura Maye, and David McGookin. 2019. Using both hands: tangibles for stroke rehabilitation in the home. In *Proceedings of the 2019 CHI conference on human factors in computing systems*. 1–14.

[25] Hand Biomechanics Lab. [n. d.]. Digit Widget. https://handbiolab.com/digit-widget/

[26] Joanne Leong, Patrick Parzer, Florian Perteneder, Teo Babic, Christian Rendl, Anita Vogl, Hubert Egger, Alex Olwal, and Michael Haller. 2016. proCover: sensory augmentation of prosthetic limbs using smart textile covers. In *Proceedings of the 29th Annual Symposium on User Interface Software and Technology*. 335–346.

[27] Hui Lin, Lin Shi, and Defeng Wang. 2016. A rapid and intelligent designing technique for patient-specific and 3D-printed orthopedic cast. *3D printing in medicine* 2 (2016), 1–10.

[28] Yuyu Lin, Jesse T Gonzalez, Zhitong Cui, Yash Rajeev Banka, and Alexandra Ion. 2024. ConeAct: A Multistable Actuator for Dynamic Materials. In *Proceedings of the 2024 CHI Conference on Human Factors in Computing Systems*. 1–16.

[29] Yuyu Lin, Hatice Gokcen Guner, Jianzhe Gu, Sonia Prashant, and Alexandra Ion. 2025. Wearable Material Properties: Passive Wearable Microstructures as Adaptable Interfaces for the Physical Environment. In *Proceedings of the 2025 CHI Conference on Human Factors in Computing Systems*. 1–16.

[30] Yiyue Luo, Kui Wu, Andrew Spielberg, Michael Foshey, Daniela Rus, Tomás Palacios, and Wojciech Matusik. 2022. Digital fabrication of pneumatic actuators with integrated sensing by machine knitting. In *Proceedings of the 2022 CHI Conference on Human Factors in Computing Systems*. 1–13.

[31] Preetham Madapura Nagaraj, Wen Mo, and Catherine Holloway. 2024. Mindfulness-based Embodied Tangible Interactions for Stroke Rehabilitation at Home. In *Proceedings of the CHI Conference on Human Factors in Computing Systems*. 1–16.

[32] Mike Nicholls, Catherine Orr, Mark Yates, and Andrea Loftus. 2008. A new means of measuring index/ring finger (2D:4D) ratio and its association with gender and hand preference. *Laterality* 13 (02 2008), 71–91. https://doi.org/10.1080/13576500701751287

[33] Jari HP Pallari, Kenneth W Dalgarno, and James Woodburn. 2010. Mass customization of foot orthoses for rheumatoid arthritis using selective laser sintering. *IEEE Transactions on Biomedical Engineering* 57, 7 (2010), 1750–1756.

[34] Fei Pan, Yilun Li, Zhaoyu Li, Jialing Yang, Bin Liu, and Yuli Chen. 2019. 3D pixel mechanical metamaterials. *Advanced Materials* 31, 25 (2019), 1900548.

[35] Dinesh K Patel, Xiaonan Huang, Yichi Luo, Mrunmayi Mungekar, M Khalid Jawed, Lining Yao, and Carmel Majidi. 2023. Highly dynamic bistable soft actuator for reconfigurable multimodal soft robots. *Advanced Materials Technologies* 8, 2 (2023), 2201259.

[36] Fang Qin, Huai-Yu Cheng, Rachel Sneeringer, Maria Vlachostergiou, Sampada Acharya, Haolin Liu, Carmel Majidi, Mohammad Islam, and Lining Yao. 2021. ExoForm: Shape Memory and Self-Fusing Semi-Rigid Wearables. In *Extended Abstracts of the 2021 CHI Conference on Human Factors in Computing Systems* (Yokohama, Japan) *(CHI EA '21)*. Association for Computing Machinery, New York, NY, USA, Article 249, 8 pages. https://doi.org/10.1145/3411763.3451818

[37] Krishnakumar Ramalingam, Lokesh Siva, Nisha Lenin, and Nandakumar Sundaramurthy. 2023. A Customised paediatric thumb web splint for management of adduction contracture of thumb. *BMJ Case Reports CP* 16, 8 (2023), e253655.

[38] Fiona Sandford, Nicola Barlow, and Jeremy Lewis. 2008. A study to examine patient adherence to wearing 24-hour forearm thermoplastic splints after tendon repairs. *Journal of Hand Therapy* 21, 1 (2008), 44–53.

[39] Mine Sarac, Massimiliano Solazzi, Edoardo Sotgiu, Massimo Bergamasco, and Antonio Frisoli. 2017. Design and kinematic optimization of a novel underactuated robotic hand exoskeleton. *Meccanica* 52 (2017), 749–761.

[40] Deborah A Schwartz and Katherine A Schofield. 2023. Utilization of 3D printed orthoses for musculoskeletal conditions of the upper extremity: A systematic review. *Journal of Hand Therapy* 36, 1 (2023), 166–178.

[41] Karin Slegers, Kristel Kouwenberg, Tereza Loučova, and Ramon Daniels. 2020. Makers in healthcare: The role of occupational therapists in the design of DIY assistive technology. In *Proceedings of the 2020 CHI Conference on Human Factors in Computing Systems*. 1–11.

[42] Kobi Steinberg, Danit Langer, Hanna Melchior, Joshua A Cohen, and Gershon Zinger. 2024. Effectiveness of the static progressive Joint Active System splint in improving upper extremity joint stiffness. *Hand Surgery and Rehabilitation* 43, 3 (2024), 101710.

[43] Rainer Storn and Kenneth Price. 1997. Differential evolution–a simple and efficient heuristic for global optimization over continuous spaces. *Journal of global optimization* 11 (1997), 341–359.

[44] Jonas Svingen, Marianne Arner, and Christina Turesson. 2023. Patients' experiences of flexor tendon rehabilitation in relation to adherence: a qualitative study. *Disability and rehabilitation* 45, 7 (2023), 1115–1123.

[45] Stavros Thomopoulos, William C Parks, Daniel B Rifkin, and Kathleen A Derwin. 2015. Mechanisms of tendon injury and repair. *Journal of Orthopaedic Research* 33, 6 (2015), 832–839.

[46] Emanuel Todorov, Tom Erez, and Yuval Tassa. 2012. MuJoCo: A physics engine for model-based control. In *2012 IEEE/RSJ International Conference on Intelligent Robots and Systems*. IEEE, 5026–5033. https://doi.org/10.1109/IROS.2012.6386109

[47] Hsin-Ruey Tsai, Chieh Tsai, Yu-So Liao, Yi-Ting Chiang, and Zhong-Yi Zhang. 2022. FingerX: Rendering Haptic Shapes of Virtual Objects Augmented by Real Objects using Extendable and Withdrawable Supports on Fingers. In *Proceedings of the 2022 CHI Conference on Human Factors in Computing Systems* (New Orleans, LA, USA) *(CHI '22)*. Association for Computing Machinery, New York, NY, USA, Article 430, 14 pages. https://doi.org/10.1145/3491102.3517489

[48] Kristin Valdes, Jessica D Boyd, Scott B Povlak, and Malgorzata A Szelwach. 2019. Efficacy of orthotic devices for increased active proximal interphalangeal extension joint range of motion: a systematic review. *Journal of Hand Therapy* 32, 2 (2019), 184–193.

[49] Jens Vertongen and Derek Kamper. 2020. Design of a 3D printed hybrid mechanical structure for a hand exoskeleton. In *Current Directions in Biomedical Engineering*, Vol. 6. De Gruyter, 20202003.

[50] Guanyun Wang, Yue Yang, Mengyan Guo, Kuangqi Zhu, Zihan Yan, Qiang Cui, Zihong Zhou, Junzhe Ji, Jiaji Li, Danli Luo, Deying Pan, Yitao Fan, Teng Han, Ye Tao, and Lingyun Sun. 2023. ThermoFit: Thermoforming Smart Orthoses via Metamaterial Structures for Body-Fitting and Component-Adjusting. *Proc. ACM Interact. Mob. Wearable Ubiquitous Technol.* 7, 1, Article 31 (mar 2023), 27 pages. https://doi.org/10.1145/3580806

[51] Qi Wang. 2016. Designing posture monitoring garments to support rehabilitation. In *Proceedings of the TEI'16: Tenth International Conference on Tangible, Embedded, and Embodied Interaction*. 709–712.

[52] Alison L Wong, Madeline Wilson, Sakina Girnary, Matthew Nojoomi, Soumyadipta Acharya, and Scott M Paul. 2017. The optimal orthosis and motion protocol for extensor tendon injury in zones IV-VIII: a systematic review. *Journal of Hand Therapy* 30, 4 (2017), 447–456.

[53] June-Tzu Yu, Yi-Chao Huang, and Chen-Sheng Chen. 2024. Research and Development of a 3D-Printed Dynamic Finger Flexion Orthosis for Finger Extension Stiffness–A Preliminary Study. *Bioengineering* 11, 4 (2024), 339.

[54] Yue-Qing Yu, Larry L Howell, Craig Lusk, Ying Yue, and Mao-Gen He. 2005. Dynamic modeling of compliant mechanisms based on the pseudo-rigid-body model. (2005).

[55] Xiaoting Zhang, Guoxin Fang, Chengkai Dai, Jouke Verlinden, Jun Wu, Emily Whiting, and Charlie CL Wang. 2017. Thermal-comfort design of personalized casts. In *Proceedings of the 30th annual ACM symposium on user interface software and technology*. 243–254.

[56] Yunbo Zhang and Tsz-Ho Kwok. 2019. Customization and topology optimization of compression casts/braces on two-manifold surfaces. *Computer-Aided Design* 111 (2019), 113–122.

[57] Clement Zheng, Zhen Zhou Yong, Hongnan Lin, HyunJoo Oh, and Ching Chiuan Yen. 2022. Shape-haptics: planar & passive force feedback mechanisms for physical interfaces. In *Proceedings of the 2022 CHI Conference on Human Factors in Computing Systems*. 1–15.

[58] J Zhu, Y Lei, A Shah, G Schein, H Ghaednia, J Schwab, et al. [n. d.]. MuscleRehab: Improving unsupervised physical rehabilitation by monitoring and visualizing muscle engagement. 2022. UIST.